IOPscience iopscience.iop.org

Home Search Collections Journals About Contact us My IOPscience

Dynamics of modified glass networks

This article has been downloaded from IOPscience. Please scroll down to see the full text article.

2000 J. Phys.: Condens. Matter 12 6979

(http://iopscience.iop.org/0953-8984/12/30/325)

View the table of contents for this issue, or go to the journal homepage for more

Download details:
IP Address: 171.66.16.221
The article was downloaded on 16/05/2010 at 06:36

Please note that terms and conditions apply.

J. Phys.: Condens. Matter **12** (2000) 6979–6989. Printed in the UK PII: S0953-8984(00)13484-8

Dynamics of modified glass networks

H Uhlig†, S Bennington†‡ and J-B Suck†

† TU Chemnitz, Institute of Physics, Materials Research and Liquids, D-09107 Chemnitz, Germany

‡ ISIS Facility, Rutherford Appleton Laboratory, Chilton, Didcot, Oxfordshire OX11 0QX, UK

Received 25 April 2000

Abstract. A comparative study of the atomic dynamics of a-$Li_2Si_2O_5$ and pure SiO_2 glass was performed using neutron inelastic scattering and applying the isotope substitution technique to suppress the coherent scattering from the network modifying Li atoms. The generalized vibrational density of states $G(\omega)$ determined in the full energy range up to 150 meV differs clearly in the high energy range and also at low energies. A strong broadening and a shift to lower energies of the sharp lines in the spectrum of SiO_2 is observed in the spectrum of the modified network glass. A detailed analysis of the measured dynamic structure factor $S(Q, \omega)$ is used to determine the change of the SiO_2 network force constants by the network modifier, which again is used to support a specific model of the modification in the Si–O network.

1. Introduction

The influence of alkali ions on the structure of the network of silica glasses has been well studied to date by x-ray and neutron diffraction. Various series of glasses [1–3] containing different alkali ions were studied. Using the isotopic substitution technique, diffraction experiments were successfully performed for glasses containing Ca or Li ions [4–6]. In spite of the fact that structural modifications are readily detectable in the total static structure factors, only a few efforts were made to detect the influence of the network modification by alkali ions on the dynamics of the network. Exceptions are the investigations of the effect of potassium ions [7] and ^{7}Li ions [8]. Here we report on an extension of the latter investigations to a much larger range of energy transfer $\hbar\omega$ and momentum transfer $\hbar Q$. The specific advantage of this experiment is the use of the isotopic substitution technique in the determination of the dynamic structure factor, i.e. the measurement of the dynamics of the modified network without coherent scattering from the network modifier. For this advantage one pays, however, with a reduction of the statistical accuracy of the data due to the high absorption cross sections of ^{6}Li for thermal neutrons using zero scattering lithium (a mixture of ^{6}Li and ^{7}Li ions) as the network modifier. Thus only the atomic dynamics of the modified SiO_2 network is investigated in the coherent part of the scattered intensity. Pure SiO_2 has successfully been investigated in a large region of Q–ω-space before [9, 10]. The structural units of silica glasses are SiO_4 tetrahedra connected to each other by shared oxygen corners. This is suggested by a value of nearly 2 which is found for the number of nearest Si–O neighbours, Z_{SiO}. This value indicates almost full connectivity. The average bond angle is about 144° with a distribution of 25° (FWHM). This value is not affected by the introduction of network modifiers [5].

0953-8984/00/306979+11$30.00 © 2000 IOP Publishing Ltd

2. Theoretical background

In neutron inelastic scattering experiments, the intensity $I(\boldsymbol{k}_0, \boldsymbol{k})$ of the scattered neutrons is measured as a function of the wave vector of the neutron before ($\boldsymbol{k}_0$) and after scattering ($\boldsymbol{k}$). From these, the momentum transfer $\hbar\boldsymbol{k}$ and the energy transfer $\hbar\omega$ are calculated here for isotropic (amorphous) samples. From the scattered intensity, the double differential cross section $\mathrm{d}^2\sigma/\mathrm{d}\Omega\,\mathrm{d}E$ is extracted after the correction and normalization procedures have been carried out. From this the dynamical structure factor $S(Q, \omega)$ can be calculated:

$$S(Q, \omega) = \frac{4\pi k_0}{\sigma^{sc} k} \frac{\mathrm{d}^2\sigma}{\mathrm{d}\Omega\,\mathrm{d}E}. \tag{1}$$

For a sample made up of several elements the total scattering cross section σ^{sc} is the concentration weighted sum of the coherent and incoherent scattering cross section.

The experimentally accessible total $S(Q, \omega)$ is the weighted sum of the partial dynamic structure factors $S_{ij}(Q, \omega)$ and the self-term of the dynamic structure factors:

$$S(Q, \omega) = \frac{4\pi}{\sigma^{sc}_{coh}} \sum_{i,j}^{n} b_i b_j c_i c_j S_{ij}(Q, \omega) + \frac{1}{\sigma^{sc}_{inc}} \sum_{i}^{n} \sigma_i^{inc} c_i S_i^{self}(Q, \omega) \tag{2}$$

with

$$\sigma^{sc}_{coh} = 4\pi \sum_{ij} b_i b_j c_i c_j$$

$$\sigma^{sc}_{inc} = \sum_{i} c_i \sigma_i^{inc}$$

c_i = atomic concentration of element i

b_i = bound coherent scattering length for neutron scattering of element i.

3. Experiment

3.1. Sample preparation

The sample of the composition $Li_2Si_2O_5$ was obtained using the powder route including densification before melting and homogenization. Details of the sample preparation have been given elsewhere [5]. In order to prevent crystallization, the melt was poured into a cold platinum die giving an amount of 10 g of usable material. It was analysed for composition and homogeneity by inductively coupled Ar-plasma optical emission spectrometry (ICP-OES) and x-ray fluorescence spectrometry. Commercially produced pure silica glass (Suprasil, Schott Glaswerke AG, Mainz, Germany) was used for the comparative measurements.

3.2. Scattering experiments

The scattering experiments were performed at the thermal neutron time-of-flight (TOF) spectrometer MARI at the ISIS spallation neutron source using an incident neutron energy of 220 meV. The energy resolution is about 2% of the incident energy, i.e. 4 meV. The sample was kept in a cryostat under vacuum at a temperature of 20 K to minimize the contribution of multiphonon scattering in the neutron energy loss spectra. The $Li_2Si_2O_5$ sample, the SiO_2 sample and the empty Al can were measured for 24 hours each. This set of measurements was completed with three vanadium runs for the calibration of the detectors.

The results were corrected for scattering angle and energy dependent background and absorption and the energy dependence of the detector efficiency. The resulting intensity was

normalized with the help of the vanadium calibration runs. It was not necessary to perform multiple scattering corrections because of the low scattering probability (<2%) due to the high absorption cross section of ^{0}Li in the $Li_2Si_2O_5$ sample (see section 4.2).

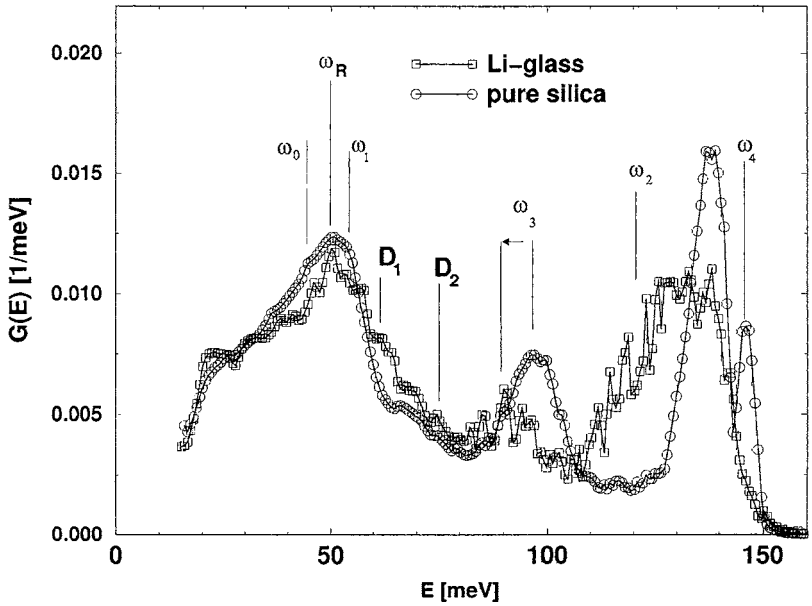

Figure 1. GVDOS of a-SiO_2 (circles) and a-$Li_2Si_2O_5$ (squares).

4. Experimental results

4.1. Generalized vibrational density of states

The normal mode analysis is made via the generalized vibrational density of states (GVDOS). This is obtained by the weighted sum of the TOF spectra and an iterative subtraction of multiphonon contributions until self-consistency was obtained. In figure 1 the GVDOSs of the glasses SiO_2 and $^0Li_2Si_2O_5$ are presented. The curve of pure silica glass (circles) agrees well with the results of Arai *et al* [10] and of a previous study [9]. In this presentation four pronounced energy bands at 50, 98, 133 and 145 meV are visible for a-SiO_2. The GVDOSs of a-$^0Li_2Si_2O_5$ (squares) and a-SiO_2 (circles) are essentially the same between 30 and 50 meV. It cannot finally be decided whether the small differences are produced by some weakness of the absorption corrections of the a-$^0Li_2Si_2O_5$ or are a result of the network modification. More pronounced deviations are detected above 40 meV and especially in the range of 90–110 meV where the expected mode at about 100 meV (a-SiO_2) is shifted towards lower energies (92 meV) for a-$^0Li_2Si_2O_5$. For this sample we can state that the incoherent contribution for ^{0}Li is 0.25 barn compared to the coherent contribution from the Si–O network of 2.83 barn. We can see a small hump in the GVDOS left from the maximum ω_R at 50 meV, at 43.3 meV (ω_0), and on the right side at 55.8 meV (ω_1). A small peak is detected at 68.5 meV. Additional small humps are found at 61 meV and 75 meV. These modes have been related to breathing modes of planar four-membered and three-membered rings [11]. The peak (ω_3) at about 100 meV (a-SiO_2) is shifted towards 90 meV for a-$Li_2Si_2O_5$. Obvious differences are observed in the range above 110 meV. Beginning with 110 meV, a broad peak with an inherent double peak

structure in the GVDOS of a-$Li_2Si_2O_5$ occurs with a maximum at 135 meV and ending at 150 meV. The GVDOS of a-SiO_2 exhibits two sharp maxima at 133 meV and at 145 meV. For further interpretation one has to keep in mind that the incoherent contribution from the Li atoms is smaller than 10% of the total scattered intensity and therefore cannot be responsible for the deviations observed. The differences found in these curves are due to the effect of the network modifier on the network neglecting the incoherent scattered contribution of the network modifier lithium. A detailed analysis of the intensities along $\omega =$ constant lines of the $S(Q, \omega =$ constant) will be necessary for a more extended interpretation. The indexing of the peaks is explained in section 5 in detail.

4.2. Total dynamic structure factors

In figure 2(a) the $S(Q, \omega)$ of a-SiO_2 is presented. The statistics is remarkably good and allows a reliable interpolation to $S(Q =$ constant, $\omega)$. The results are in good agreement with the $S(Q, \omega)$ published by Price and Carpenter [9]. Also the total dynamic structure factor $S(Q, \omega)$ of a-$Li_2Si_2O_5$ exhibits oscillations along cuts at $\omega =$ constant. However, the statistical accuracy is not of the same quality as in the case of a-SiO_2 due to the large absorption cross section of the sample. The quality of the data could not be improved by the addition of further runs but only by integrating 10 meV along the sections. The absence of intensity at about 100 meV in the case of a-$Li_2Si_2O_5$ is obvious from a comparison of the two curves in figure 3. $S(Q, \omega)$ of a-SiO_2 contains a small amount of multiple scattering which is not the case for $S(Q, \omega)$ of a-$Li_2Si_2O_5$ where lithium, acting as a strong absorber, drastically reduces the probability of multiple scattering. In order to estimate the amount of multiply scattered intensity, we assume the multiply scattered intensity to be mainly caused by double scattering processes. The ratio δ of double scattered intensity to single scattered intensity (in the quasi-isotropic approximation) for cylindrical samples is given by [12]

$$\delta = \Sigma_s \left(-\frac{d}{2} \ln \left(\frac{d}{\sqrt{(2r)^2 + d^2}} \right) + \frac{8r}{3\pi} \left(\frac{\pi}{2} - \tan^{-1} \left(\frac{2r}{d} \right) \right) \right) \tag{3}$$

with

$\Sigma_s = n\sigma_s$density of atoms $\times$ total scattering cross section

$d =$ height of the sample

$r =$ radius of the sample.

The insertion of the values $r = 2.15$ cm and $d = 6$ cm into equation (3) leads to the ratio of $\delta = 0.085$. The contribution of triple and higher order multiple scattering is usually reduced by a factor of six, so all multiple scattered intensity is slightly below 10% of all scattered intensity for a-SiO_2. Thus we have to attribute about 8% of the measured intensity to multiply scattered neutrons in the SiO_2 spectra.

4.3. Sections at constant energies

4.3.1. $E = 1.5$ meV. In figure 3 sections through $S(Q, \omega)$ at $E = 1.5$ meV are presented. The curves are the result of the addition of three adjacent spectra except at $S(Q, 0)$, where the spectra were contaminated by some remaining Bragg peaks of the aluminum cylinders. Thus these curves essentially represent the structure of $S(Q)$. Reasonable values are found for $Q > 1.5$ Å^{-1}, therefore a detailed investigation of the region of the first sharp diffraction peak is not possible here. The maxima located at about $Q = 2.5$ Å^{-1} and $Q = 5.0$ Å^{-1} are well pronounced in both curves. The structure of these curves agrees well with that of the

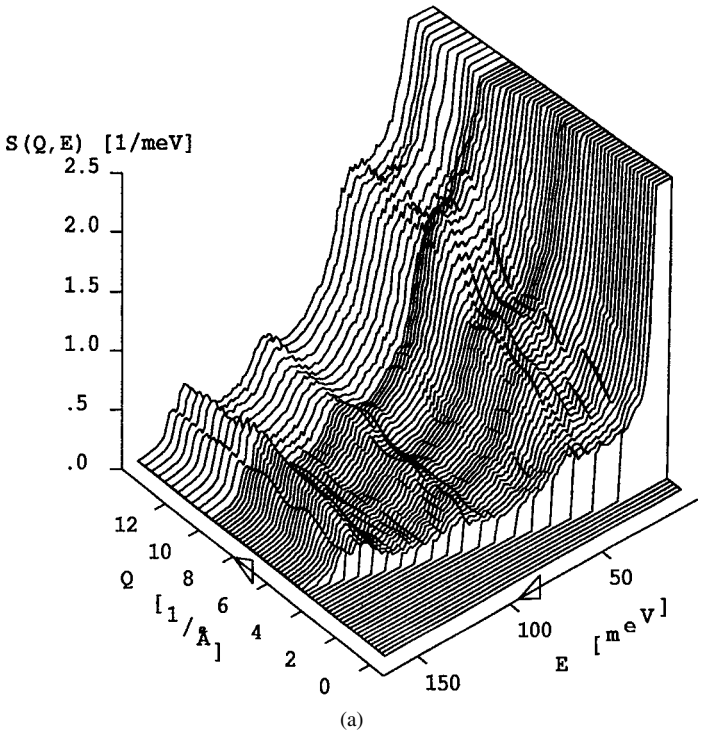

(a)

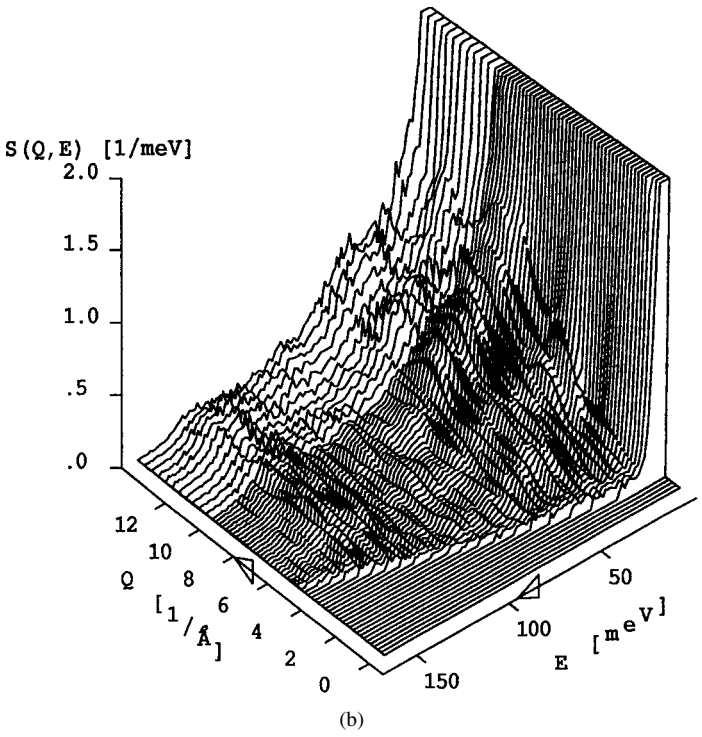

(b)

Figure 2. (a) 3D representation of the total dynamic structure factor $S(Q, \omega)$ of a-SiO_2 measured at 20 K. (b) 3D representation of the total dynamic structure factor $S(Q, \omega)$ of a-$Li_2Si_2O_5$ measured at 20 K.

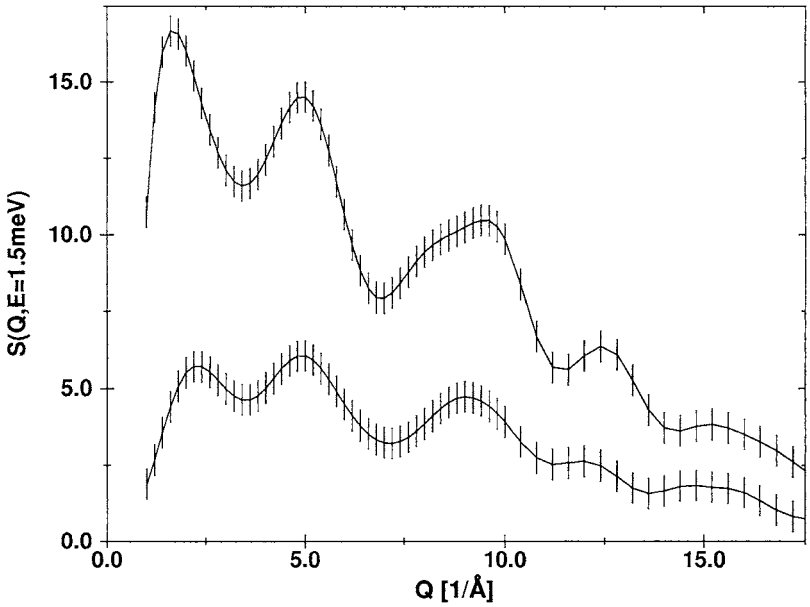

Figure 3. Total dynamic structure factors $S(Q, \hbar\omega = 1.5$ meV) of amorphous SiO_2 (upper curve) and a-$Li_2Si_2O_5$ (lower curve).

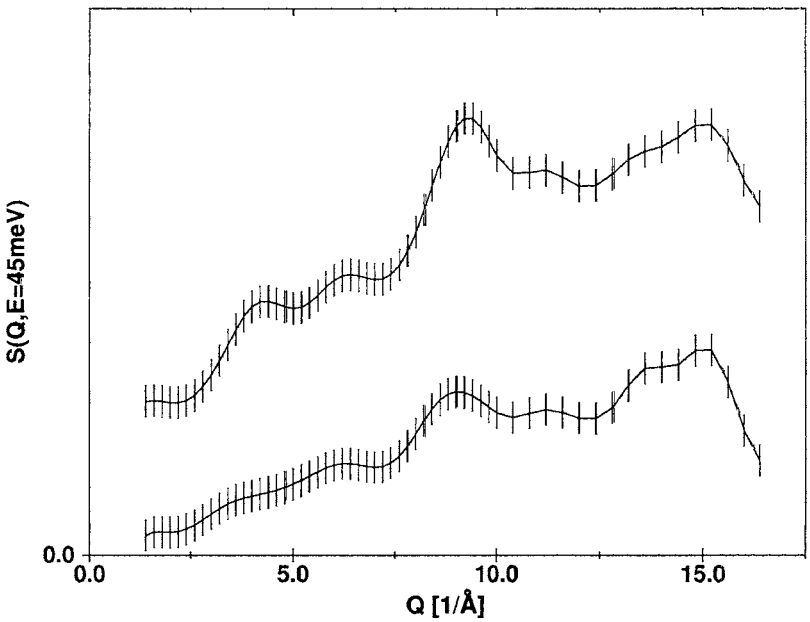

Figure 4. Total dynamic structure factors $S(Q, \hbar\omega = 45$ meV) of amorphous SiO_2 (upper curve) and a-$Li_2Si_2O_5$ (lower curve).

static structure factors $S(Q)$ [5]. The two weak maxima in the region between 8 and 10 $Å^{-1}$ expected from the diffraction experiment could not be well resolved in this inelastic neutron scattering experiment which has a coarse Q-resolution for intensity reasons compared with

normal diffraction experiments. The maxima at about 12.5 $Å^{-1}$ and the small humps at 15 $Å^{-1}$ agree with the maxima in $S(Q)$ from diffraction experiments [5].

4.3.2. $E = 45$ meV. From the GVDOS shown in figure 1, the region between $\hbar\omega = 40$ and 50 meV is expected to carry similar vibrational modes in both glasses. In figure 4 we present the intensity obtained by integrating $S(Q, \omega)$ from 40 to 50 meV indicated with the mean value of 45 meV. The similarities are obvious for the presented Q-range with the restriction that the oscillations in the curve of a-$Li_2Si_2O_5$ are less pronounced compared to those of a-SiO_2 especially at Q-values below 7.5 $Å^{-1}$.

4.3.3. $E = 68.5$ meV. The two curves of figure 5 are rather similar in their shape. The most important difference is that the maximum visible at 9.15 $Å^{-1}$ for a-SiO_2 is shifted to 8.6 $Å^{-1}$ for a-$Li_2Si_2O_5$. The maximum located at 11.2 $Å^{-1}$ is clearly visible in the case of a-$Li_2Si_2O_5$. It may be overlapped by the tail of the broad maximum located at 9.15 $Å^{-1}$ and is therefore not well separated in the case of a-SiO_2. A further maximum is visible for both curves at about 14.3 $Å^{-1}$, which is more pronounced in the curve of a-$Li_2Si_2O_5$.

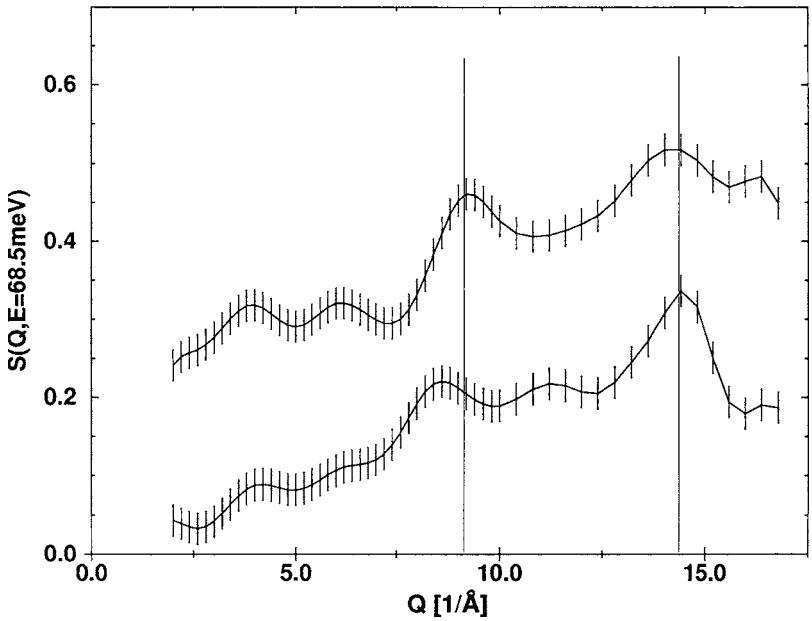

Figure 5. Total dynamic structure factors $S(Q, \hbar\omega = 68.5\,\text{meV})$ of amorphous SiO_2 (upper curve) and a-$Li_2Si_2O_5$ (lower curve).

4.3.4. $E = 100$ meV. The cuts through $S(Q, \omega)$ near $\hbar\omega = 100$ meV (see figure 6) were obtained by integrating $S(Q, \omega)$ from 95 to 105 meV. The two cuts show a strong similarity in the Q-range from 5 up to 15 $Å^{-1}$ even though the structure in the curve is less pronounced in the case of the $Li_2Si_2O_5$ glass. Further we observe a shift of the maximum located at 9.5 $Å^{-1}$ in $S(Q, 100\,\text{meV})$ of a-SiO_2 towards 8.5 $Å^{-1}$ in that of a-$Li_2Si_2O_5$.

4.3.5. $E = 120$ meV. The GVDOS for a-SiO_2 as presented in figure 1 indicates a low intensity in the energy region of 120 meV. In contrast for a-$Li_2Si_2O_5$ we found a comparatively high

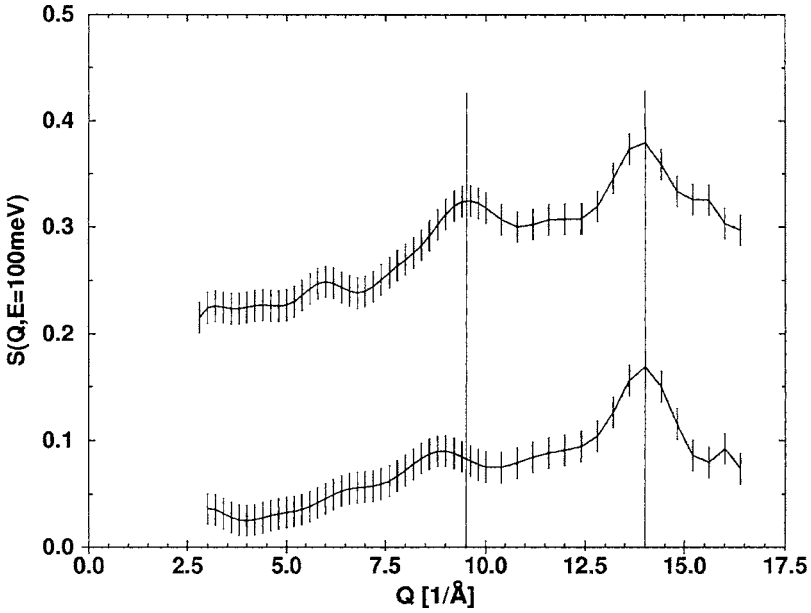

Figure 6. Total dynamic structure factors $S(Q, \hbar\omega = 100$ meV) of amorphous SiO_2 (upper curve) and a-$Li_2Si_2O_5$ (lower curve).

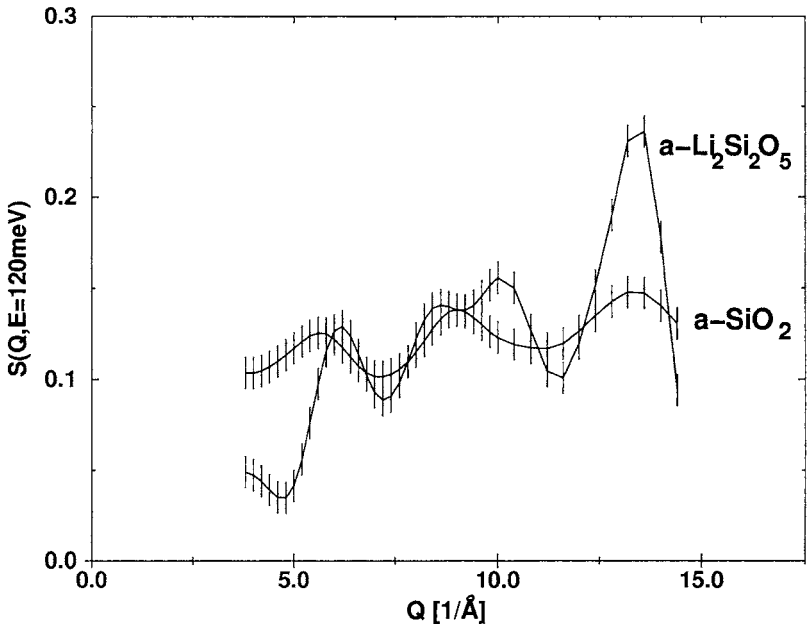

Figure 7. Total dynamic structure factors $S(Q, \hbar\omega = 120$ meV) of amorphous SiO_2 and a-$Li_2Si_2O_5$.

intensity together with pronounced maxima in $S(Q, \hbar\omega = 120$ meV) (see figure 7). This observation justifies the assumption of a mode at 120 meV, which could be the antisymmetric stretching mode which is expected in this energy region.

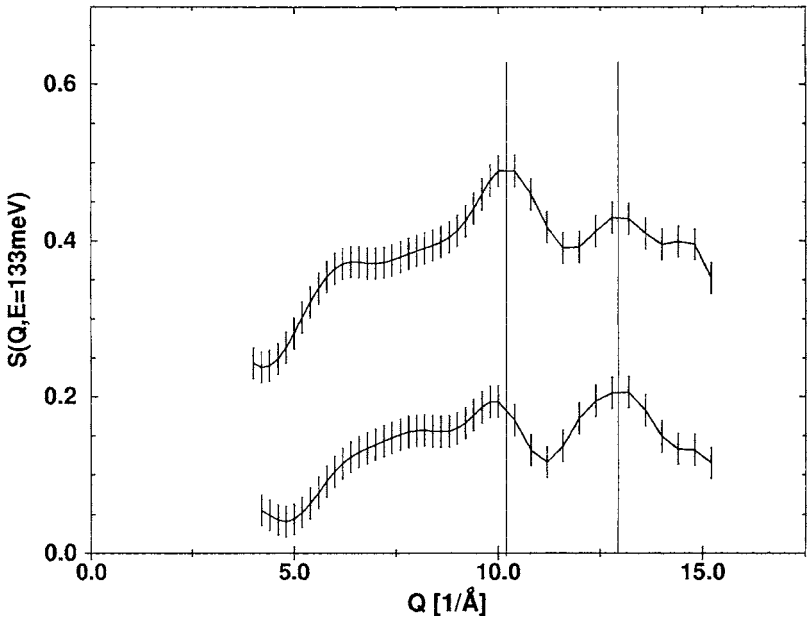

Figure 8. Total dynamic structure factors $S(Q, \hbar\omega = 133$ meV) of amorphous SiO_2 (upper curve) and a-$Li_2Si_2O_5$ (lower curve).

4.3.6. $E = 133$ meV. In figure 8 the cuts through $S(Q, \omega)$ of the samples continue to differ at the most pronounced maximum, now located right from 10.2 $Å^{-1}$ for a-SiO_2 and 9.8 $Å^{-1}$ for a-$Li_2Si_2O_5$, which is less pronounced here. The maximum at 13 $Å^{-1}$ is not shifted for the $Li_2Si_2O_5$ glass but is slightly more pronounced and broadened.

5. Discussion

The aim of this investigation was to study the influence of a network modifier (lithium ions) on the short range dynamics of the Si–O network. The starting point of this discussion is therefore the static structure of the two samples. In the experimentally determined pair distribution functions one observes only some small changes in the first coordination sphere of Si with increasing Li content. Especially the shape of the Si–O pair correlation is not affected by increasing the Li_2O content [5]. However, the average O–O distance of the first coordination sphere is slightly elongated with increasing Li content. It varies from 2.60 Å (SiO_2) up to 2.64 Å for a-$Li_2Si_2O_5$. This tendency has been found by several authors [1, 5] and can be understood in terms of a softening of the Si–O bonds of non-bridging oxygens.

The breathing mode of the SiO_4 tetrahedron is observable in the region of 50 meV in the GVDOS (see figure 1). The intensity is reduced and the peak is broadened for the $Li_2Si_2O_5$ glass, which indicates also a softening of the Si–O bond in the tetrahedra for non-bridging oxygens.

Since the Q–ω range is related to the short range structure of the network we will discuss the results in the light of the central force model derived by Sen and Thorpe [13]. In figure 9, the assumed short range order of a common AX_2 network is drawn schematically. The structural unit is an AX_4 tetrahedron with corner sharing X atoms. All A–X distances are the same and all X–A–X angles have the value of 109.5°. The symbol SS stands for the symmetric

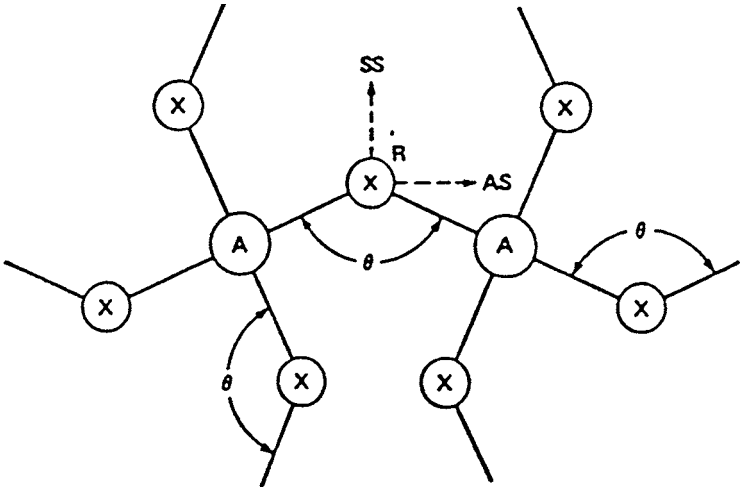

Figure 9. Explanations of the motions in an AX_2 network [14]. The X-atom motions shown are defined as symmetric stretch (SS), antisymmetric stretch (AS) and rocking (R) modes.

stretch mode, AS for the antisymmetric stretch mode and R stands for the rocking mode perpendicular to the AXA plane. Although there is some weakness in the application of this model, as the explanation of reasonable values for the intertetrahedral angle θ fails, this model is useful for the interpretation of neutron scattering data as well as Raman spectra. The further interpretation of the data uses the concepts presented by Galeener *et al* [14]. Equation (4) was first derived by Kulas and Thorpe [15] and is used for the estimation of the non-central force constant β. Equations (5)–(8) are the band limit formulas for central forces only, derived by Sen and Thorpe [13]. This model excludes all non-central forces from the consideration. Also excluded from this model is the special ring statistics and a certain statistical distribution of the dihedral angle. Only the masses of the participating atoms and the intertetrahedral angle θ are included in this model. This set of equations describes the dynamics common to AX_2 glasses [16]:

$$\omega_0^2 = 2\beta/m_X \tag{4}$$

$$\omega_1^2 = (\alpha/m_X)(1+\cos\theta) \tag{5}$$

$$\omega_2^2 = (\alpha/m_X)(1-\cos\theta) \tag{6}$$

$$\omega_3^2 = (\alpha/m_X)(1+\cos\theta) + 4\alpha/3m_A \tag{7}$$

$$\omega_4^2 = (\alpha/m_X)(1-\cos\theta) + 4\alpha/3m_A. \tag{8}$$

Galeener [17] used this set of equations for the estimation of the force constants and the bond angles. Using equations (5) and (7) one obtains

$$\alpha = (\omega_3^2 - \omega_1^2)(3m_A/4) \tag{9}$$

$$\cos(\theta) + 1 = \omega_1^2(\omega_3^2 - \omega_1^2)^{-1}(4m_x/3m_A). \tag{10}$$

The value of ω_0 was taken from the small hump on the left of the main peak ω_R. For the further assignment of the frequencies ω_i see [14]. Although this model does not give the precise values for θ, we want to use it in order to estimate the force constants α and β.

The constant β for non-central forces is independent of the Li content in the glass.

Using the values of ω_3 and ω_1 from the GVDOS we can calculate the central force constant α. The values obtained (see table 1) indicate a softening with increasing Li content. We

Table 1. Calculated force constants α, β and intertetrahedral angle θ using ω_i values as measured for SiO_2 and $^0Li_2Si_2O_5$ glasses.

	$\hbar\omega_0$ [meV]	$\hbar\omega_1$ [meV]	$\hbar\omega_2$ [meV]	$\hbar\omega_3$ [meV]	$\hbar\omega_4$ [meV]	α [N m^{-1}]	β [N m^{-1}]	θ
SiO_2	43.3	55.8	—	98.8	145	549	58	131.7
$^0Li_2Si_2O_5$	43.3	55.8	120	90.5	—	412	58	122.4

assume that the softening is caused by non-bridging oxygen atoms because Si–O–Si bonds are highly covalent, while the Li–O–Si bonds for non-bridging oxygen have partially ionic character. Therefore, a softening of these bonds is observed, which is accompanied by a slight elongation of the Si–O bonds with increasing Li content. From the dynamic structure factor presented in figures 2–8 we can conclude that these changes are not the result of numerous new vibrational modes. The $S(Q, \omega = \text{constant})$ cuts have largely the same structure for a-SiO_2 and a-$Li_2Si_2O_5$.

The lower intensity at the position of ω_4 (LO mode) can be discussed in the light of the decreasing degree of connectivity in the network of a $Li_2Si_2O_5$ network. As result of the decrease of the connectivity, the AS (antisymmetric stretching, see figure 9) mode becomes possible, especially in the case of non-bridging oxygen atoms.

5.1. Conclusions

The change of the short range dynamics of the SiO_2 networks with increasing Li content is reflected in the GVDOS. The intensity shifts observed here are used to calculate the force constants of the model applied. A softening of the Si–O bonds is observed together with an increasing intensity for the antisymmetric stretching mode and a decreasing intensity at the LO mode for a-$Li_2Si_2O_5$. These results are in good agreement with those of neutron diffraction experiments, where a slight elongation of Si–O bonds is observed together with the decrease of the degree of connectivity of the SiO network with increasing Li content. For further details computer simulations will be needed.

References

[1] Waseda Y 1980 *The Structure of Non Crystalline Materials* (New York: McGraw-Hill)
[2] Yasui I, Hasegawa H and Imaoka M 1983 *Phys. Chem. Glasses* **24** 65
[3] Misawa M, Price D L and Suzuki K 1980 *J. Non-Cryst. Solids* **37** 85
[4] Gaskell P H 1993 *Proc. ILL/ESRF Workshop on Methods in the Determination of Partial Structure Factors* ed J-B Suck, P Chieux, D Raoux and C Riekel (Singapore: World Scientific)
[5] Uhlig H, Hoffmann M J, Bellissent R, Lamparter H P, Aldinger F and Steeb S 1996 *J. Am. Ceram. Soc.* **79** 2833
[6] Zhao J, Gaskell P H and Soper A K 1998 *J. Non-Cryst. Solids* **232–234** 721
[7] Dove M T, Harris M H, Hannon A C, Parker J M, Swainson I P and Gambhir M 1997 *Phys. Rev. Lett.* **78** 1070
[8] Uhlig H, Mentese S, Longeville S and Suck J-B 1999 submitted
[9] Price D L and Carpenter J M 1987 *J. Non-Cryst. Solids* **92** 153
[10] Arai M, Hannon A C, Otomo T, Hiramatsu A and Hishiima T 1995 *J. Non-Cryst. Solids* **192/193** 230
[11] Galeener F L 1982 *Solid State Commun.* **44** 1037
[12] Sears V F 1975 *Adv. Phys.* **24** 1
[13] Sen P N and Thorpe M F 1977 *Phys. Rev.* B **15** 4030
[14] Galeener F L, Leadbetter A J and Stringfellow M W 1983 *Phys. Rev.* B **27** 1052
[15] Kulas R and Thorpe M F 1976 *Structure and Excitations of Amorphous Solids, Proc. 176th Williamsburg Meeting Division Struct. Excitation Amorphous Solids Am. Phys. Soc.* ed G Lucovsky and F L Galeener (New York: AIP)
[16] Bell R J, Dean P and Hibbins-Butler D C 1970 *J. Phys. C: Solid State Phys.* **3** 2111
[17] Galeener F L 1979 *Phys. Rev.* B **19** 4292